Targeted cell elimination reveals an auxin-guided biphasic mode of lateral root initiation

Peter Marhavý,[1,6] Juan Carlos Montesinos,[1] Anas Abuzeineh,[2,3,7] Daniel Van Damme,[2,3] Joop E.M. Vermeer,[5] Jerôme Duclercq,[2,3,8] Hana Rakusová,[1] Petra Nováková,[1,6] Jiři Friml,[1] Niko Geldner,[4] and Eva Benková[1]

[1]Institute of Science and Technology Austria (IST Austria), 3400 Klosterneuburg, Austria; [2]Department of Plant Systems Biology, Vlaams Instituut voor Biotechnologie (VIB), 9052 Gent, Belgium; [3]Department of Plant Biotechnology and Bioinformatics, Ghent University, 9052 Gent, Belgium; [4]Department of Plant Molecular Biology, Biophore, UNIL-Sorge, University of Lausanne, 1015 Lausanne, Switzerland; [5]Plant Cell Biology, Department of Plant and Microbial Biology, University of Zürich, 8008 Zürich, Switzerland

To sustain a lifelong ability to initiate organs, plants retain pools of undifferentiated cells with a preserved proliferation capacity. The root pericycle represents a unique tissue with conditional meristematic activity, and its tight control determines initiation of lateral organs. Here we show that the meristematic activity of the pericycle is constrained by the interaction with the adjacent endodermis. Release of these restraints by elimination of endodermal cells by single-cell ablation triggers the pericycle to re-enter the cell cycle. We found that endodermis removal substitutes for the phytohormone auxin-dependent initiation of the pericycle meristematic activity. However, auxin is indispensable to steer the cell division plane orientation of new organ-defining divisions. We propose a dual, spatiotemporally distinct role for auxin during lateral root initiation. In the endodermis, auxin releases constraints arising from cell-to-cell interactions that compromise the pericycle meristematic activity, whereas, in the pericycle, auxin defines the orientation of the cell division plane to initiate lateral roots.

[*Keywords*: lateral root organogenesis; mechanical forces; meristem proliferation activity; auxin]

Supplemental material is available for this article.

Received December 23, 2015; revised version accepted December 30, 2015.

The processes by which multicellular organisms take shape result from the tight coordination of cell division, elongation, and differentiation. Although the principal mechanisms of cell cycle control are common to all eukaryotic organisms, plant organogenesis is unique. Whereas the complete animal body plan is typically established during embryogenesis, most plant organs are initiated de novo during post-embryonic growth. Within a single organism, different organogenic programs are activated, including those for lateral roots, shoots, leaves, and flowers, all conditioned by a spatiotemporally tight coordination of cell division and patterning. Such post-embryonic organogenesis requires the division processes to be strictly controlled through yet to be revealed mechanisms.

In plant roots, the pericycle cell file is a unique example of a meristematic tissue that, despite its partial differentiation, remains competent to divide and differentiate and, ultimately, give rise to new organs (Malamy and Benfey 1997; Laplaze et al. 2005; Dubrovsky et al. 2011). In the model plant *Arabidopsis thaliana*, pericycle cells adjacent to the xylem are activated at regular spatiotemporal intervals to undergo formative anticlinal divisions, launching the lateral root developmental program. Among the regulatory programs that coordinate initiation of the lateral root organogenesis (De Smet et al. 2006; Dubrovsky et al. 2008; Laskowski et al. 2008; Moreno-Risueno and Benfey 2011; Lucas et al. 2013; Marhavý et al. 2013; Beeckman and De Smet 2014; Vermeer et al. 2014), local communication between pericycle and adjacent endodermal cells emerges as an important control point in the recruitment of founder cells (FCs) for initiation of the lateral

Present addresses: [6]Department of Plant Molecular Biology, Biophore, UNIL-Sorge, University of Lausanne, 1015 Lausanne, Switzerland; [7]Department of Molecular Biology and Ecology of Plants, Tel Aviv University, Tel Aviv 69978, Israel; [8]Université de Picardie Jules Verne, 80025 Amiens, France.
Corresponding author: eva.benkova@ist.ac.at
Article is online at http://www.genesdev.org/cgi/doi/10.1101/gad.276964.115.

root developmental program (Marhavý et al. 2013; Vermeer et al. 2014). The endodermis might play a role in building the local maxima of the phytohormone auxin in the pericycle cells needed for their specification to become FCs and transition to the next developmental phase. The auxin efflux carrier PIN-FORMED3 (PIN3), transiently expressed in endodermal cells adjacent to FCs, was found to facilitate the auxin reflux required for the FC establishment (Marhavý et al. 2013). Importantly, lateral root primordia, which gradually expand from the moment of initiation, have spatial demands that must be accommodated through tight interaction with the overlaying tissues. Recent reports hint at a role played by auxin in these aspects of lateral root organogenesis and reveal an unexpected importance of this regulatory path. Findings that expression of several cell wall remodeling genes is specific to endodermal cells above initiated primordia (Swarup et al. 2008) and that tissue-specific suppression of the auxin signaling in the endodermis severely compromises lateral root initiation and development (Lucas et al. 2013; Vermeer et al. 2014) strongly support the model in which auxin-driven morphogenetic modulations are directly engaged in the control of lateral root organogenesis. However, how the endodermis contributes to the regulation of the early lateral root initiation phase and which processes of the initiation are governed through interaction with the endodermis remain largely unknown. Here we show that the proliferative activity of the pericycle, the tissue that gives rise to lateral organs and hence models the whole root system architecture, is constrained through an interaction with the adjacent endodermis. The physical elimination of endodermal cells releases the pericycle cells from their cell cycle arrest, but auxin is indispensable to determine the proper orientation of the cell division plane during the subsequent divisions and thereby delineates the lateral root developmental program.

Results

Ablation of endodermal cells interferes with the orientation of FC divisions

To gain insight into the regulatory role of the endodermis in the early phases of lateral root initiation, we established a platform for targeted ablation of specific root cells. Disruption of the target cells by ultraviolet (UV) laser resulted in a rapid and specific internalization of propidium iodide (PI), indicative of cell death (Fig. 1A). Importantly, none of the neighboring cells were damaged by the ablation of different cell types, such as endodermal (Fig. 1B,C) or cortex (Fig. 1D,E) cells, confirming the highly cell-specific nature of the approach. Combining the laser ablation platform with real-time imaging enabled us to investigate the developmental impact of these ablations on lateral root initiation and organogenesis.

Auxin accumulation in pericycle cells adjacent to the xylem pole is one of the earliest hallmarks of specification of pericycle cells to FCs, which then undergo a series of anticlinal divisions with respect to the primary root axis, thus giving rise to stage I lateral root primordia (Malamy and Benfey 1997; Dubrovsky et al. 2008). To monitor simultaneously auxin responses and cell division patterns during the early phases of the lateral root initiation, we used the transgenic line expressing both the auxin-sensitive reporter *DR5pro::N7:Venus* (Ulmasov et al. 1997; Heisler et al. 2005) and the microtubule reporter consisting of the microtubule-binding domain (MBD) of *MICROTUBULE-ASSOCIATED PROTEIN4* (*MAP4*) fused to the GFP driven by the constitutive *35S* promoter (Marc et al. 1998). As expected, after the pericycle cells had acquired their FC identity, correlating with an increase of the *DR5* reporter expression, they underwent a series of anticlinal cell divisions, giving rise to stage I lateral root primordia. Under our experimental conditions, we detected 4.64 ± 0.48 anticlinal divisions prior to the first periclinal division, implying transition to the next developmental phase of lateral root organogenesis (Fig. 2A).

To assess the role of the endodermis during the early phases of lateral root initiation, we specifically removed the endodermal cells adjacent to the FCs. Endodermal cell ablation (ECA) adjacent to FCs did not prevent cell cycle progression, and the FCs underwent, on average, 3.4 ± 0.22 divisions ($n = 20$ ablation events) within 15 h after ablation (Fig. 2B,D,E). However, in contrast to the stereotypical formative FC divisions that are exclusively anticlinal with respect to the primary root axis (Fig. 2A), the FC divisions were oriented periclinally (2.5 ± 0.17 of the 3.4 ± 0.22 divisions) after ECA (Fig. 2B,D). To rule out that atypical division patterns observed after ECA were caused by a microtubule cytoskeleton malfunction in constitutively MAP4-GFP reporter-expressing plants, we used the *PIN3::PIN3-GFP* membrane-located reporter and the *AUR1::RFP-MBD* reporter composed of the RFP fused to the MAP4 MBD under control of the *AURORA1* promoter (Van Damme et al. 2011) for monitoring the FC responses to ECA. Both reporters confirmed the periclinal orientation of the ECA-triggered FC divisions (Supplemental Figs. S1A,B,D). These findings indicate that physical elimination of endodermal cells does not preclude FC divisions but alters their division plane orientation.

Ablation of endodermal cells activates naive pericycle cell divisions

Lateral root initiation is tightly linked with auxin, and its accumulation in the xylem pole pericycle cells correlates with their FC identity acquisition and subsequent lateral root initiation. The inactive or so-called naive pericycle cells remain silent and do not proceed to lateral root organogenesis. To examine the ECA impact on naive pericycle cells without acquired FC identity, we applied the ECA in the vicinity of pericycle cells lacking *DR5* auxin reporter expression. Notably, the ECA triggered cell divisions of the adjacent pericycle cells independently of detectable auxin activity in the pericycle cells before and for 15 h after ablation (Fig. 2C). Real-time monitoring of naive pericycle cells after ablation revealed that nearly all ECA-activated divisions were periclinal. On average, 2.9 ± 0.19 divisions were detected in a 15-h time window

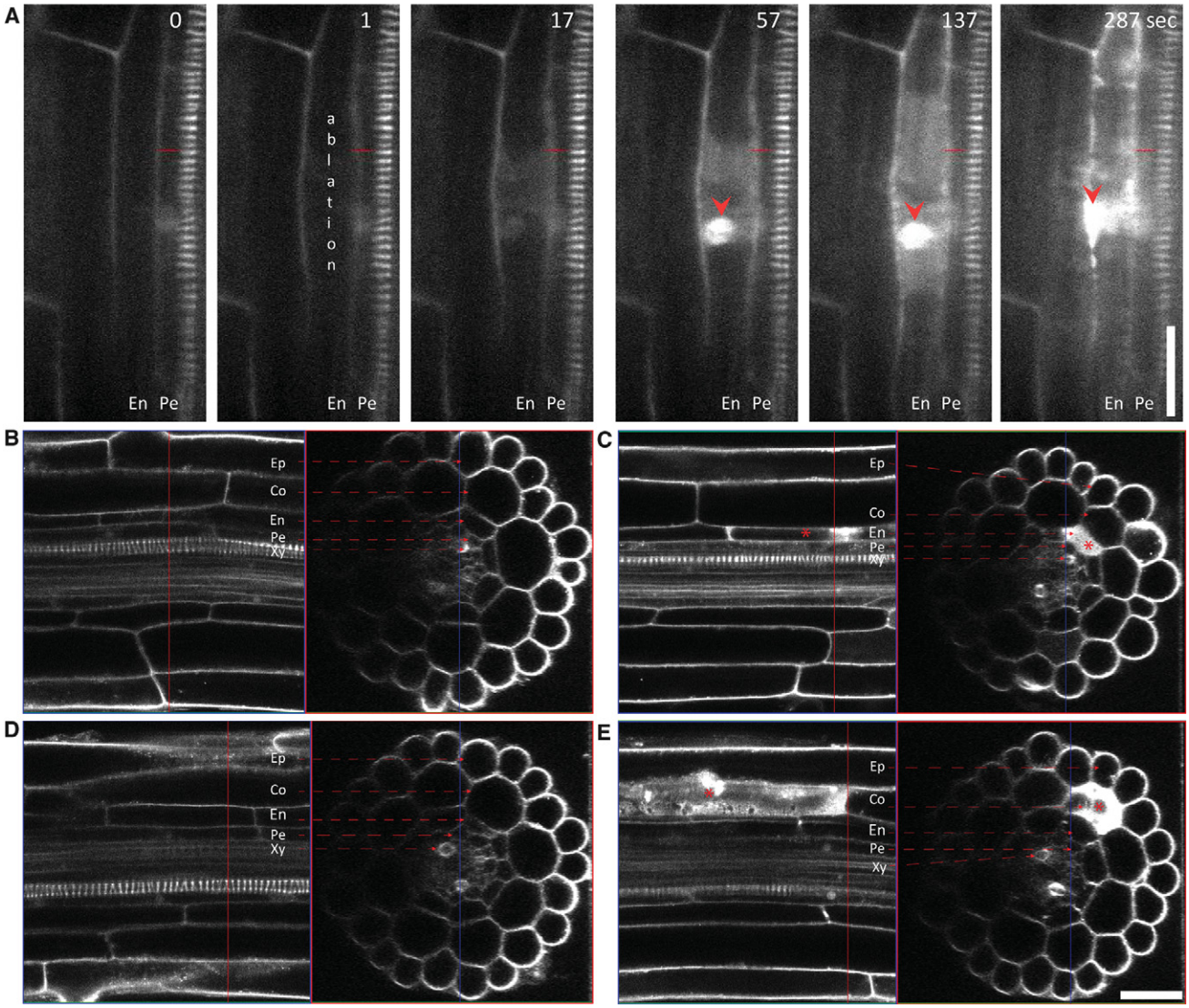

Figure 1. Locally specific ablation of root cells. (*A*) Ablation of endodermal cells leading to rapid penetration of PI (white) into the ablated endodermal cells and staining of the nucleus (red arrowhead), indicating cell death. (*B–E*) Exclusive PI accumulation in laser-ablated cells. The endodermal (*C*) or cortex (*E*) cell after ablation (red star) accumulates PI (white), indicating cell death. Longitudinal and transversal confocal *z*-sectioning and three-dimensional reconstruction of roots prior to (*B*,*D*) and 287 sec after (*C*,*E*) ablation. A red asterisk marks the ablated cell. Live-imaging time points are indicated in the *top right* corner of each frame. Experiments were done with the *DR5pro::N7:Venus/PIN3::PIN3-GFP* line. The PIN3-GFP membrane reporter in combination with PI staining enabled visualization of root cell files. (Co) Cortex; (En) endodermis; (Ep) epidermis; (Pe) pericycle; (Xy) xylem. Bar, 30 µm.

after ECA ($n = 20$ ablation events), of which 2.6 ± 0.18 divisions occurred periclinally with respect to the primary root growth axis (Fig. 2D).

In *Arabidopsis*, lateral roots initiate repetitively in an acropetal manner so that new primordia are positioned distally to the older lateral branches. This acropetal pattern of lateral root initiation implies that pericycle cells located at the distal root end within a so-called developmental window exhibit the highest probability to initiate a lateral root, whereas, in the proximal root part, the probability of pericycle cells undergoing division ceases, correlating with the low frequency of lateral root initiation (Dubrovsky et al. 2006, 2011). Consistently, lateral root initiations are rarely found in the proximity of existing lateral root primordia (Dubrovsky et al. 2000). To test whether the responses to ECA of pericycle cells differ depending on their position along the primary root axis, we applied ECA in the proximal root zone across the existing lateral root primordia. Ablations of these endodermal cells resulted in the activation of periclinal divisions in adjacent naive pericycle cells (Supplemental Fig. S1C,D). The average number of divisions triggered by ECA in the proximal root zone did not differ statistically from the average number of pericycle cell divisions occurring after ECA in the developmental window of the root zone (Supplemental Fig. S1E).

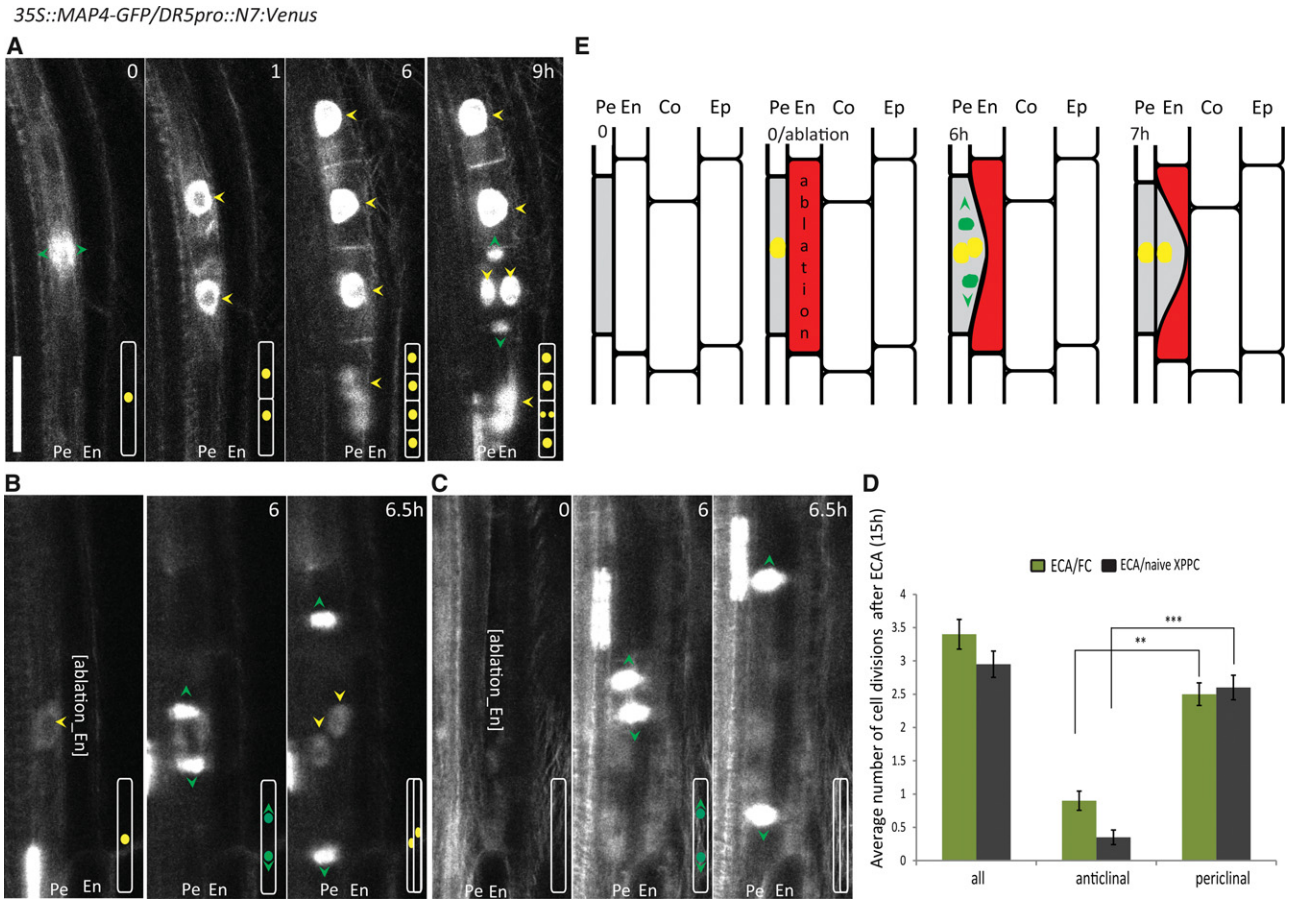

Figure 2. Division of adjacent pericycle cells triggered by ablation of endodermal cells. (*A–C*) Real-time monitored lateral root initiation (*A*) and FC (*B*) and naive xylem pole pericycle cell (XPPC) (*C*) division after ablation of the adjacent endodermal cell. Microtubule *35S::MAP4-GFP* and the auxin-sensitive *DR5pro::N7:Venus* reporters were used to visualize the direction of cell plate expansion (green arrowheads) and the auxin activity in the nucleus (yellow arrowheads), respectively. (*A*) FCs (time 0) undergo anticlinal divisions to produce four initial cells of lateral root primordia (time 1 and 6 h) prior to the first periclinal division (9 h). FCs expressing the *DR5pro::N7:Venus* reporter (*B*) as well as naive xylem pole pericycle cells in which no *DR5pro::N7:Venus* reporter expression could be detected (*C*) divide periclinally after ablation of endodermal cells. Schematic representations of the cell divisions are shown in the *bottom right* corners. (*D*) Quantification of the number of divisions occurring for 15 h after endodermal cell ablation (ECA) above FCs or naive xylem pole pericycle cells. The average number of total and anticlinal versus periclinal divisions per ablation event was scored. (**) $P < 0.001$; (***) $P < 0.0001$. $n = 20$ ablation events. Error bars indicate the standard error of the mean. (*E*) Scheme of the ECA-triggered division of pericycle cells. ECA (red) above the pericycle cells (gray) triggers periclinal divisions of the pericycle cells. Green arrowheads and green circles indicate the direction of cell plate expansion as monitored by *35S::MAP4-GFP*, and yellow circles indicate nuclei expressing the *DR5pro::N7:Venus* auxin reporter. The image series depicted are representative examples of at least 20 observations. Live-imaging time points are indicated in the *top right* corner of each frame. Bar, 30 µm.

Our results indicate that the endodermis might effectively restrain the meristematic activity of the pericycle. Attenuation of these restraints by physical disruption of endodermal cells stimulates the meristematic activity of any xylem pole pericycle cell regardless of its position along the root axis and the auxin response.

Ablation of nonendodermal root cell types does not stimulate pericycle cell divisions

To examine whether other root cell types might also be controlled by the interaction with adjacent tissues, as the observed pericycle cell division ability after ECA, we removed different cell types in fully differentiated root parts and monitored the behavior of adjacent cells. Ablation of either xylem or cortex cells did not trigger cell divisions in adjacent pericycle cells (Fig. 3A) in either adjacent endodermal or epidermal cells (Fig. 3C), respectively. Similarly, ablation of differentiated epidermal cells could not activate division of neighboring cortex cells (Fig. 3D). On that account, the endodermis–pericycle interaction seems to be unique in restricting the meristematic activity of the pericycle cells (Fig. 3B), and the possibility that the ablation of either epidermal or cortex cells induces production of a non-cell-autonomous signal that might trigger pericycle proliferative activity can be excluded.

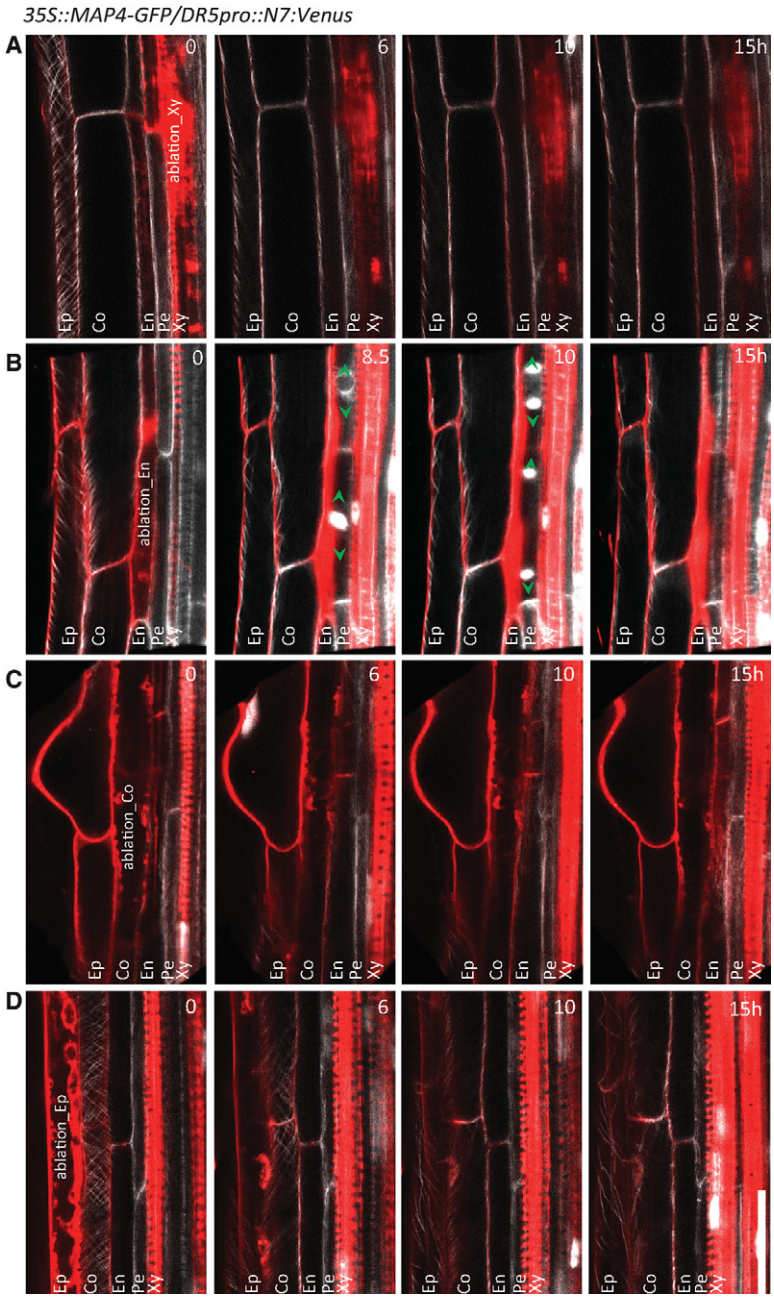

Figure 3. Lack of stimulation of pericycle cell divisions by ablation of nonendodermal root cell types. (*A–D*) No divisions detected in pericycle cells or any of the neighboring cells in the mature parts of the main root by ablation of differentiated xylem (*A*), cortex (*C*), or epidermal (*D*) cells when compared with ablation of endodermal cells that activates periclinal division of adjacent pericycle cells (*B*). The reporters *35S::MAP4-GFP* for microtubules (white) and auxin reporter *DR5pro::N7:Venus* expressed in nuclei as well as PI counterstaining (red) were used to visualize cells and the orientation of cell plate expansion in dividing cells (green arrowheads). The image series depicted are representative examples from at least 10 observations. Live-imaging time points are indicated in the *top right* corner of each frame. Bar, 30 µm.

ECA-triggered pericycle cell divisions occur independently of auxin signaling and transport

Auxin is a well-established trigger of lateral root organogenesis, and its accumulation in pericycle cells is required for FC specification and transition to stage I (Dubrovsky et al. 2008; Marhavý et al. 2013). ECA activated divisions of adjacent pericycle cells, although no auxin response could be detected in these cells (Fig. 2C; Supplemental Fig. S1C), implying that the mechanisms underlying the ECA-triggered pericycle cell divisions might differ from auxin-induced divisions during lateral root initiation. To test whether the pericycle cell divisions after ECA depend on the functional auxin perception and signaling, we examined roots of the triple mutant deficient in multiple auxin receptors, including *TRANSPORT INHIBITOR1* (*TIR1*), *AUXIN SIGNALING F-BOX2* (*AFB2*), and *AFB3* (*tir1 afb2 afb3*) (Dharmasiri et al. 2005; Kepinski and Leyser 2005; Chen et al. 2014) as well as the *solitary root/indole-3-acetic acid14* (*slr/iaa14*) mutant (Fukaki et al. 2002, 2005; Vanneste et al. 2005), both of which are severely affected in lateral root initiation and development. ECA in either the *slr* or the *tir1 afb2 afb3* mutant triggered periclinal divisions of pericycle cells despite the repressed auxin signaling pathway (2.45 ± 0.15 and 1.8 ± 0.2 divisions within 15 h, $n = 20$, respectively) (Fig. 4A,B,D). Similarly, auxin transport inhibition by 1-*N*-naphthylphthalamic acid (NPA), which completely

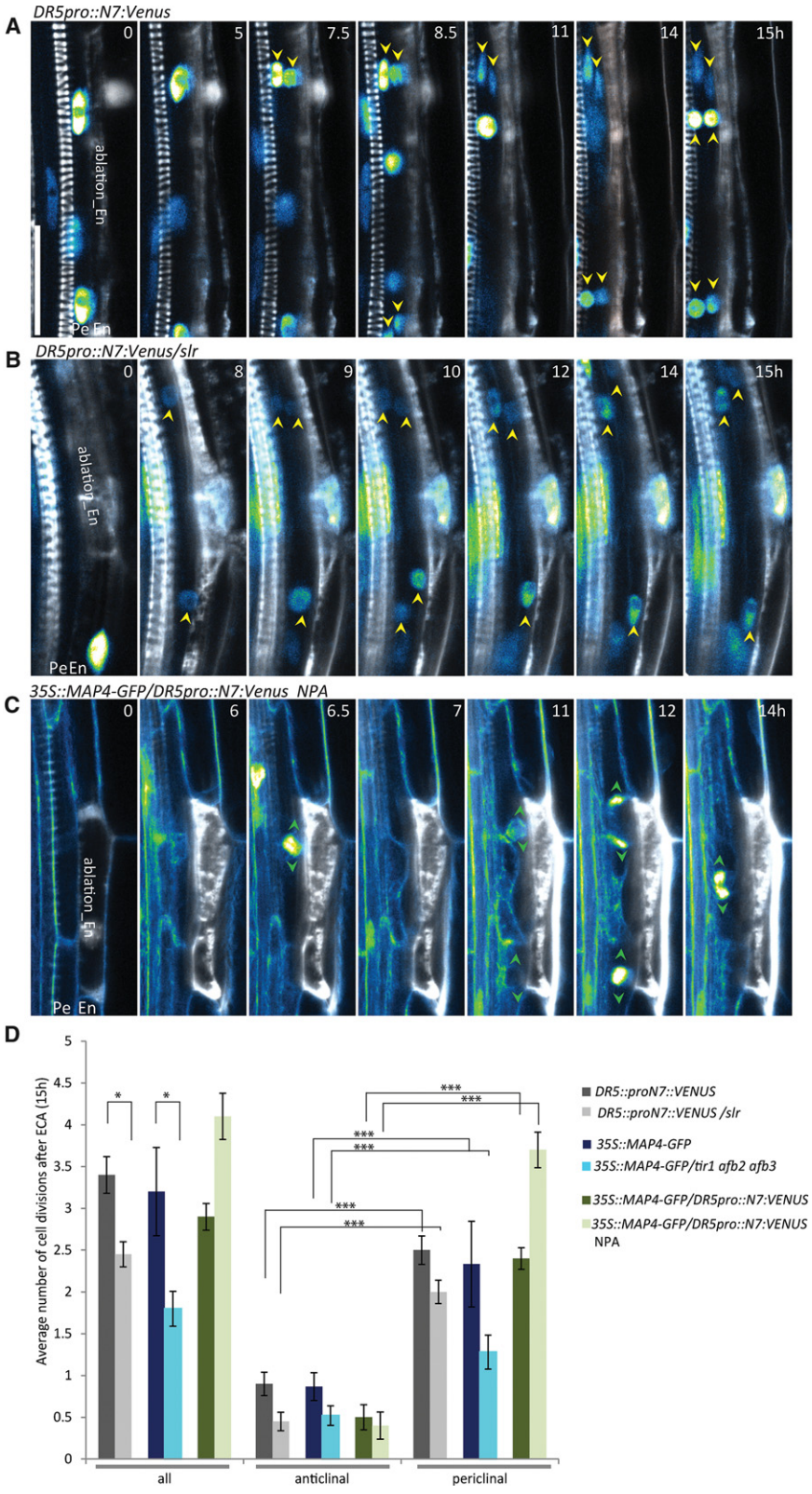

Figure 4. Pericycle cell divisions triggered by ablation of adjacent endodermal cells occurring independently of auxin signaling and transport. (*A–C*) Ablation of endodermal cells triggering periclinal division of pericycle cells in control roots (*A*), *slr* mutant roots (*B*), and roots grown on 5 µM NPA, a polar auxin transport inhibitor (*C*). Cell divisions were visualized with the *DR5pro::N7:Venus* auxin reporter labeling the nuclei (*A–C*), the *35S::MAP4-GFP* (green) microtubule marker (*C*), and PI (white) counterstaining (*A–C*). (*A*,*B*) Yellow arrowheads indicate nuclei expressing *DR5pro::N7:Venus* after division. (*C*) Green arrowheads mark the cell plate expansion direction visualized by the *35S::MAP4-GFP* reporter. (*D*) Quantification of the number of divisions occurring for 15 h after ECA above the pericycle cells in *slr* and *tir1 afb2 afb3* mutant auxin signaling backgrounds and seedlings grown on 5 µM NPA in comparison with the respective controls. The average number of total and anticlinal versus periclinal divisions per ablation event was scored. Error bars indicate the standard error of the mean. (*) $P < 0.05$; (***) $P < 0.0001$. $n = 20$ ablation events. Live-imaging time points are given in the *top right* corner of each frame. Bar, 30 µm.

impedes lateral root initiation (Casimiro et al. 2001), did not prevent the ECA-triggered pericycle cell divisions (Fig. 4C,D). Notably, the reduced number of divisions observed in auxin perception and signaling mutants after ECA suggests that the auxin signaling pathway in the pericycle contributes to maintenance of its basal proliferation ability.

Previous studies demonstrated that inhibition of the auxin signaling pathway in endodermal cells by tissue-specific expression of the *short hypocotyl2-2* (*shy2-2*)/*iaa3* repressor mutant under control of the Casparian strip membrane domain protein (CASP) promoter severely affects lateral root initiation (Vermeer et al. 2014). ECA in *CASP::shy2-2* roots activated divisions of adjacent pericycle cells similarly to the control, indicating that physical elimination of the endodermal cells might compensate for the lack of auxin activity in these cells (Supplemental Fig. S2A–C). Hence, ablation of endodermal cells can bypass the auxin activity-based stimulation of cell cycle re-entrance of pericycle cells.

ECA triggers pericycle cell swelling and activates expression of cell cycle regulatory genes

To progress toward formative cell divisions, FCs undergo cell shape modulation characterized by a volume increase (Fig. 5A; Vermeer et al. 2014). To examine whether the FC volume of the pericycle cells also increased in response to ECA, we determined the width of the pericycle cells before ablation and shortly before occurrence of the first division. Ablation of endodermal cells was accompanied by a significant increase in the pericycle cell width (Fig.

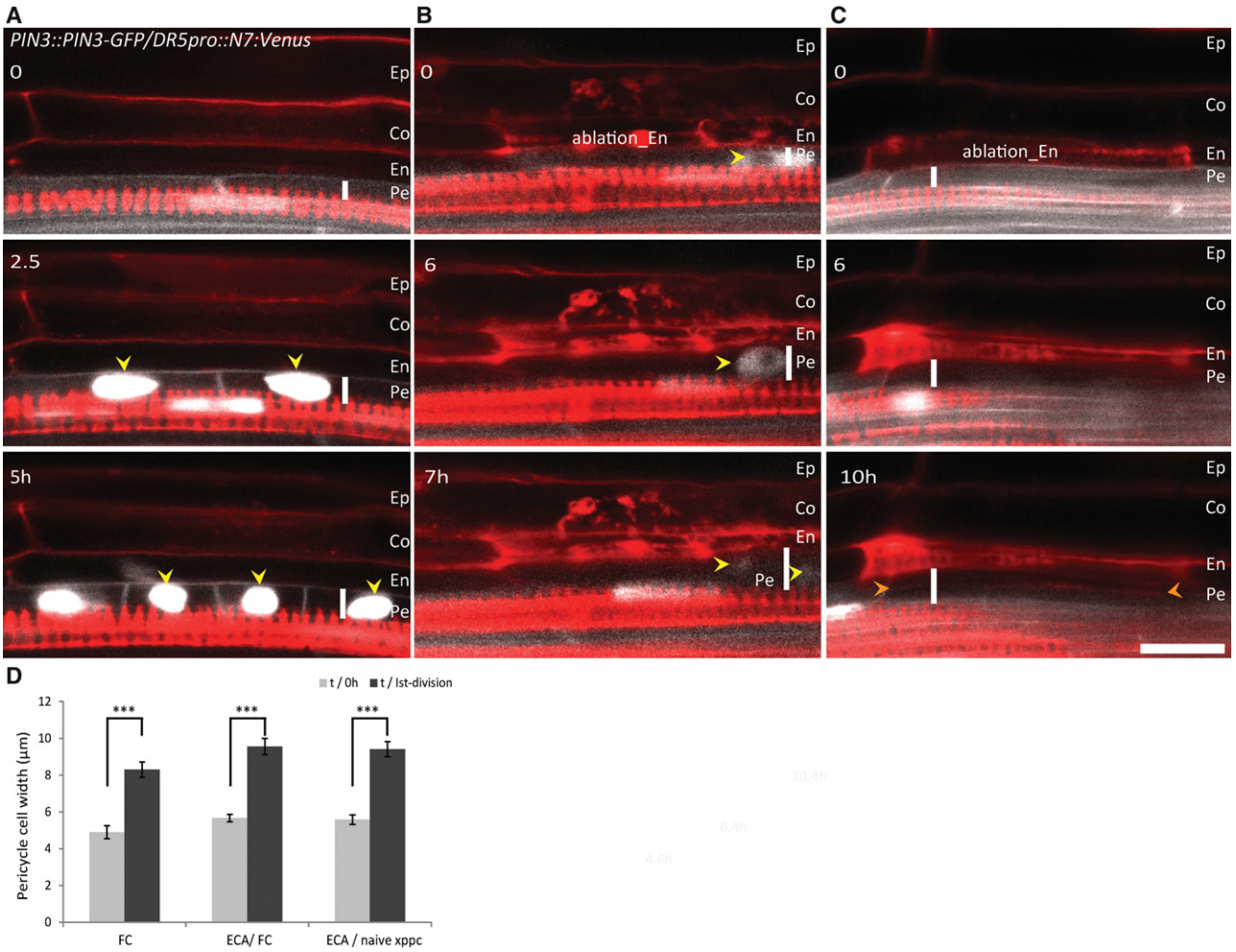

Figure 5. Increased pericycle cell width after adjacent ECA. (*A–C*) Visualization of the increased pericycle cell volume prior to division. (*A*) Pericycle cells that acquired FC identity and expressed the *DR5pro::N7:Venus* auxin reporter expand prior to division. ECA above either FCs (*B*) or naive xylem pole pericycle cells (XPPCs) (*C*) results in pericycle cell swelling. The *PIN3::PIN3-GFP* membrane reporter (white), the *DR5pro::N7:Venus* auxin reporter (nucleus localized, white), and counterstaining with PI (red) were used for real-time visualization. (*A–C*) Vertical white lines indicate the width of the pericycle cells. Yellow arrowheads point to nuclei expressing the *DR5pro::N7:Venus* auxin reporter, and orange arrowheads indicate newly formed cell membranes after division. (*D*) Quantification of the pericycle cell width before and at the moment of the first division. Error bars indicate the standard error of the mean. (***) $P < 0.0001$. $n = 10$ events. Live-imaging time points are indicated in the *top left* corner of each frame. Bar, 30 µm.

5B–D). These data are in agreement with previous observations (Vermeer et al. 2014) and demonstrate that an increase of cell volume precedes pericycle cell divisions. Thus, ablation of endodermal cells triggers swelling of the pericycle cells independently of the auxin signaling.

To investigate the ECA effect on the meristematic activity in adjacent pericycle cells, we monitored the expression of the B-type *CYCLIN1* gene that marks cells in the G2-to-M transition phase and is frequently used as reporter for lateral root initiation (Colón-Carmona et al. 1999; Beeckman et al. 2001). The *CycB1;1::GUS* and *CycB1;1::GFP* reporters were expressed in the dividing pericycle cells after ECA, thus confirming that endodermis disruption activated the cell cycle machinery in adjacent pericycle cells (Supplemental Fig. S3A,B,E,F). The cell cycle was restricted to the cells directly underneath the ablated endodermal cells, indicating that local endodermal cell disruption, rather than a long-distance nonautonomous signal, initiates the process. Expectedly, treatment with hydroxyurea (HU), a cell cycle inhibitor (Young and Hodas 1964), severely inhibited the pericycle cell divisions despite ECA (Supplemental Fig. S3C,D,G). Altogether, the results show that the endodermis imposes an important regulatory function to coordinate the cellular activity of the pericycle linked with its entrance into the lateral root developmental program, such as volume increase and activation of the cell cycle machinery.

ECA-triggered pericycle cell divisions do not result in the formation of lateral root primordia

Lateral roots initiate by a series of 4.64 ± 0.48 ($n = 20$) consecutive divisions that occur in an exclusively anticlinal manner (Malamy and Benfey 1997; our observations). Although ECA triggers divisions of pericycle cells, their orientation does not correspond to typically formative divisions observed during initiation of lateral root primordia. To examine whether ECA-triggered cell divisions might nevertheless result in the formation of lateral root primordia ectopically, we monitored the markers exhibiting specific expression patterns in lateral root primordia 22 h and 5 d following ablation. The *SCARECROW* (*SCR*) gene is expressed in stage II lateral root primordia, marking endodermal cells in developing primordia (Supplemental Fig. S4A; Marhavý et al. 2013). The expected *SCR::SCR-YFP* expression pattern exhibited in control primordia could not be detected in the conical structure that was formed as result of the ECA-triggered pericycle cell divisions (Supplemental Fig. S4B). Likewise, expression of the *GAL4-GFP* enhancer trap-based *J1103* reporter that is expressed specifically from stage II lateral root primordia onward (Bielach et al. 2012) did not occur in these structures (Supplemental Fig. S4D,E). An auxin response maximum that is required for proper organogenesis of lateral root primordia (Benková et al. 2003) and can be monitored by the *DR5* auxin reporter was also not found in the structure formed above FCs after ECA (Supplemental Fig. S5A,B). In contrast, expression of the xylem pole pericycle cell *GAL4-GFP* enhancer trap-based reporter *J0121* was maintained in the daughter cells of dividing naive pericycle cells, hinting at a proliferative character of the ECA-triggered divisions (Supplemental Fig. S5D,E). Altogether, these data demonstrate that ECA-activated pericycle cell divisions are not formative and do not lead to lateral root organogenesis.

Auxin determines the cell division plane orientation in dividing pericycle cells

Organogenesis of lateral root primordia results from a highly stereotypical pattern of cell divisions and subsequent differentiation (Malamy and Benfey 1997). Although physical removal of the endodermal cells by ECA resets the meristematic activity of pericycle cells independently of auxin, we found that it cannot drive the lateral root developmental program. The periclinal, instead of anticlinal, orientation of pericycle cell divisions did not comply with proper formation of lateral root primordia. Hence, we hypothesized that auxin might be required to determine the formative division orientations. To test the impact of auxin, we examined the ECA-triggered pericycle cell divisions in roots treated with exogenous auxin. Surprisingly, auxin application had a significant effect on the orientation of the cell division plane. In the presence of auxin, ECA-triggered pericycle cell divisions occurred preferentially in an anticlinal, instead of a periclinal, orientation (Fig. 6A,B; Supplemental Fig. S6A,B). On average, 2.4 ± 0.15 anticlinal divisions ($n = 20$ ablation events) were observed in roots treated with auxin versus 0.9 ± 0.14 in untreated control roots (Fig. 6E; Supplemental Fig. S6C). To investigate whether an increase in endogenous auxin levels would also affect the orientation of pericycle cell divisions after ECA, we analyzed the *yucca* gain-of-function mutant (Zhao et al. 2001; Cheng et al. 2006). As with the auxin treatment, the proportion of anticlinal divisions occurring in pericycle cells after ECA in the *yucca* background was significantly higher than that in control roots (Supplemental Fig. S6D–F). Altogether, these data show that, during the early phases of lateral root initiation, auxin in pericycle cells might play a specific role in determining the division plane orientation.

Auxin-driven reorientation of the pericycle divisions requires functional auxin perception and microtubule dynamics

Auxin signaling and perception mutants were examined to investigate the molecular requirements of the auxin-mediated periclinal-to-anticlinal reorientation of the pericycle divisions after ECA. In the *slr/iaa14* mutant, which is defective in auxin signal transduction, auxin promoted a periclinal-to-anticlinal reorientation of the division plane comparable with that of the control (Supplemental Fig. S7A–E). However, in the *tir1 afb2 afb3* auxin perception mutant, auxin was significantly less efficient in the anticlinal positioning of pericycle cell divisions after ECA, pointing to the involvement of the TIR1 (AFB)-dependent perception in this process (Supplemental Fig. S7E).

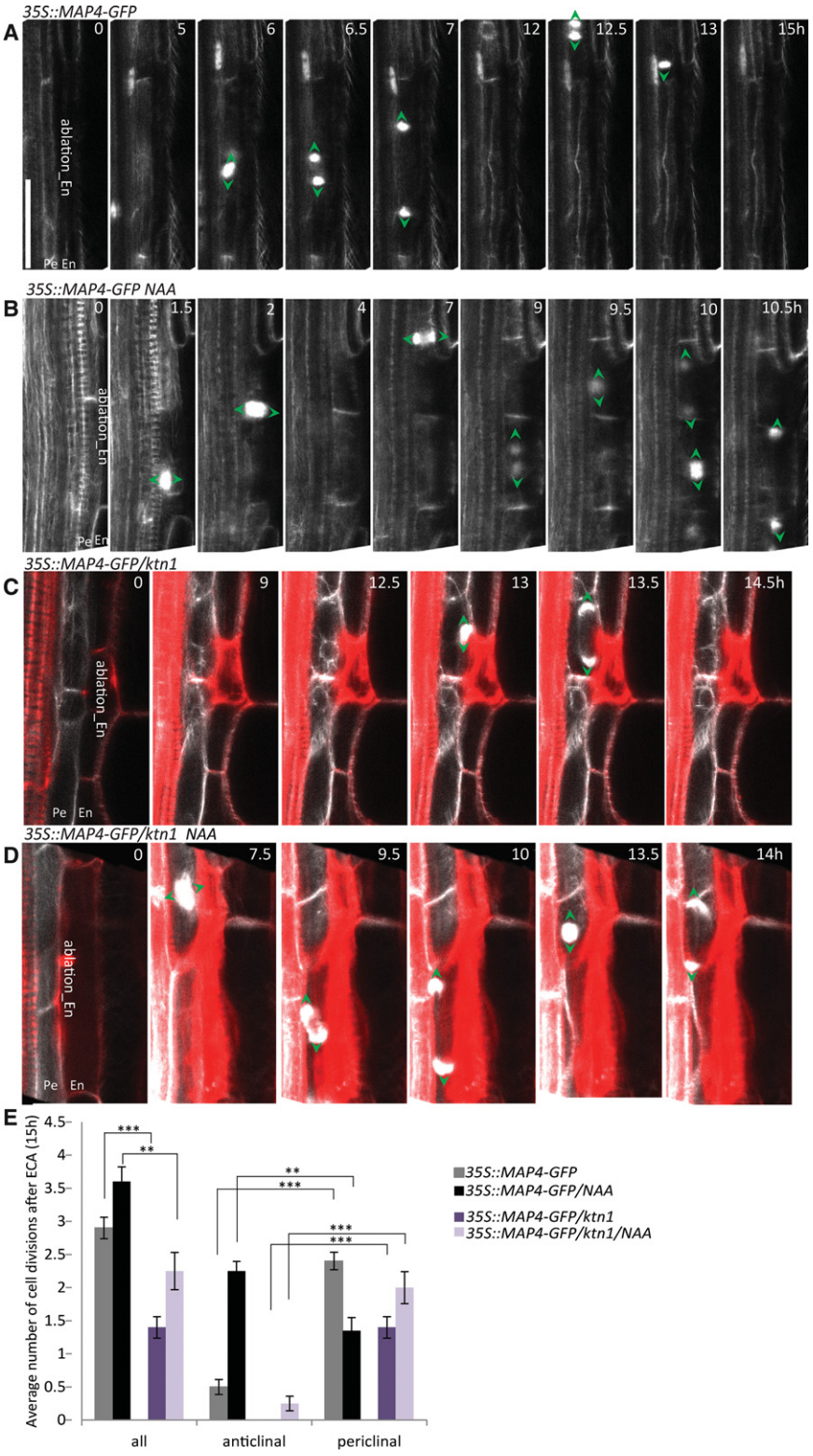

Figure 6. Cell division plane orientation in dividing pericycle cells determined by auxin and the functional cytoskeleton. (*A*, *C*) Periclinal division of adjacent pericycle cells triggered by ECA in control roots and the *katanin1* (*ktn1*) microtubule-severing factor mutant (shown in *C*). (*B*,*D*) Anticlinally oriented pericycle cell divisions were determined by auxin (0.1 µM 1-naphthaleneacetic acid [NAA]) after ECA (*B*), whereas the *ktn1* mutant is largely insensitive to auxin-mediated anticlinal divisions after ECA (*D*). The direction of the cell plate expansion during cell divisions was visualized with the *35S::MAP4-GFP* reporter (green arrowheads). (*E*) Quantification of the number of divisions occurring for 15 h after ECA in control *35S::MAP4-GFP* and *35S::MAP4-GFP/ktn1* seedlings with and without NAA treatment. The average number of total and anticlinal versus periclinal divisions per ablation event was scored. Error bars indicate the standard error of the mean. (**) $P < 0.001$; (***) $P < 0.0001$. $n = 20$ ablation events. Live-imaging time points are indicated in the *top right* corner of each frame. Bar, 30 µm.

Among the cellular components decisive for the cell division plane orientation, the microtubule cytoskeleton plays a dominant function (Hamada 2014). In plant cells, auxin induces robust rearrangements of the cortical microtubule cytoskeleton (Fischer and Schopfer 1997; Takesue and Shibaoka 1999; Vineyard et al. 2013; Chen et al. 2014). This auxin activity depends on the TIR1 (AFB) perception (Chen et al. 2014) and is largely compromised in the mutant lacking the microtubule-severing factor KATANIN1 (KTN1) (Burk et al. 2001; Uyttewaal et al.

2012; Chen et al. 2014). To explore whether the specification of auxin-governed formative divisions involves an interaction with the microtubule cytoskeleton, we applied ECA in the KTN1-defective mutant. Although ECA triggered pericycle divisions in *ktn1* seedlings, pericycle cells were delayed in their response to ECA and frequently exhibited aberrant oblique division patterns (Fig. 6C–E). Noteworthy, *ktn1* mutants exhibited a reduced sensitivity to auxin, and periclinal cell divisions prevailed also in the presence of auxin after ECA (Fig. 6D,E). Altogether, these data indicate that a dynamic microtubule cytoskeleton is an important component of the auxin-driven framework that specifies formative division plane orientations in the pericycle cells, thereby launching the lateral root organogenesis.

Formative divisions reset by auxin launch the lateral root developmental program

Whether auxin-driven anticlinal divisions of pericycle cells were sufficient to reset lateral root organogenesis was studied by monitoring the expression of the reporters *SCR::SCR-YFP*, *J1103*, and *DR5pro::N7:Venus*, which exhibit specific patterns during primordia development (Supplemental Fig. S4A,C). Twenty-two hours and 48 h after ECA in the presence of auxin, *SCR::SCR-YFP* expression was detected in dividing pericycle cells. The *SCR-YFP* signal was located in the outer cells of the dividing structure, indicative of cell differentiation and patterning linked with the *SCR* activity during lateral root organogenesis (Supplemental Fig. S4C; Marhavý et al. 2013). Similarly, the reporter expression of *J1103* as well as *DR5pro::N7:Venus* was recovered after ECA in the presence of auxin in a pattern resembling that found in normally developing lateral root primordia (Supplemental Figs. S4F, S5C). Hence, unlike proliferative divisions observed in pericycle cells after ECA, in which none of these markers were expressed (Supplemental Figs. S4B,E, S5B), auxin addition is sufficient to guide these cells through a series of formative divisions that might delineate the lateral root developmental program.

Discussion

Molecular mechanisms that control initiation and formation of new organs is a central theme in developmental biology. The unique nature of the plant body architecture that results from continuous post-embryonic organ formation implies that these mechanisms can delicately integrate division and differentiation processes during the plant life cycle. Pericycle cell files are an example of a plant tissue in which tightly spatiotemporally confined meristematic activity determines the formation of lateral organs and hence the whole root system architecture. Although the pericycle serves as the source tissue for FC recruitment for all lateral root organs, the molecular mechanisms that underlie the spatiotemporally tightly controlled specification and subsequent reactivation of the meristematic activity remain largely unknown. The direct regulatory function of the overlaying endodermis in the control of lateral root initiation is a newly emerging concept based on recent findings demonstrating that FCs and developing lateral root primordia tightly communicate with adjacent tissues, including endodermis (Swarup et al. 2008; Lucas et al. 2013; Marhavý et al. 2013; Vermeer et al. 2014). Coordinated with the FC specification, the genetic network that is activated is composed of auxin transporters, auxin signaling components, and cell wall remodeling genes in the endodermal cells adjacent to the FCs (Swarup et al. 2008; Lucas et al. 2013; Marhavý et al. 2013; Vermeer et al. 2014), pointing out that adjacent tissues encounter an important regulatory function during formation of new lateral organs. However, how the endodermis is engaged in the onset of the lateral root initiation process and control of the lateral root development is scarcely understood. Establishment of the ablation platform enabled us to address these issues and revealed unexpected facts on the intertissular interactions for the FC recruitment and delineation of the lateral root organogenesis. We found that the endodermis inhibits the meristematic activity of the pericycle. Mechanical removal of the endodermis releases this constraint, and pericycle cells proceed through the cell cycle. Notably, all pericycle cells at the xylem pole, independently of auxin and regardless of its position along the primary root, respond to the removal of the adjacent endodermis, indicating that all pericycle cells possess an intrinsic capacity to divide but are limited in their ability to do so by the attached endodermis. Re-entrance of pericycle cells into the cell cycle after ablation of neighboring endodermal cells is accompanied by an increase in cell volume, corresponding to the endodermis function that restricts the pericycle cell cycle progression via cell enlargement. Disengagement from the constraints administrated by the endodermis on pericycle cells seems to be one of the critical steps during early lateral root initiation that might be coordinated by auxin under physiological conditions. Although physical disruption of the endodermis is sufficient to trigger the meristematic activity of the pericycle, it does not suffice to set up formative divisions and delineate the lateral root developmental program. We found that auxin is the factor indispensable for these key elements of the lateral root organogenesis. The reduced auxin responsiveness of pericycle cells deprived of endodermal control in mutants defective in auxin perception and microtubule dynamics suggests that the TIR1/AFB receptor-mediated perception and functional microtubule cytoskeleton are components of the auxin-driven framework that specifies formative divisions in the pericycle, thereby launching the lateral root organogenesis.

Based on our observations, we propose that auxin plays a dual spatially and temporally distinct role in coordinating lateral root initiation. First, auxin activity in the endodermis coordinates the release of the mechanical constraints that normally inhibit the meristematic pericycle activity, thus enabling pericycle cells to re-enter the cell cycle. Subsequently, its activity in the dividing pericycle cells is required to define the formative anticlinal cell divisions to follow the lateral root organogenesis program.

Materials and methods

Plant material

The following transgenic *A. thaliana* (L.) Heynh. lines have been described elsewhere: *DR5pro:N7:Venus* (Heisler et al. 2005), *SCR::SCR-YFP* (Heidstra et al. 2004), *PIN3::PIN3-GFP* (Žádníková et al. 2010), *J1103*, *J0121* (Nottingham *Arabidopsis* Stock Centre (http://nasc.nott.ac.uk/), *35S::MAP4-GFP* (Marc et al. 1998), *CYC B 1;1::GUS* (Colón-Carmona et al. 1999), *CYC1;1B::GFP* (Ubeda-Tomás et al. 2009), *UBQ::Wave131-YFP* (Geldner et al. 2009), *UBQ::Wave131-YFP/CASP::shy2-2* (Vermeer et al. 2014), *Yucca1D* (Cheng et al. 2006), and *35S::MAP4-GFP/ktn1* (Chen et al. 2014). The lines *35S::MAP4-GFP/DR5pro:N7:Venus*, *DR5pro:N7:Venus/slr*, *35S::MAP4-GFP/tir1afb2afb3,* and *PIN3::PIN3-GFP/Yucca1D* were generated by crosses. The *pAUR1::RFP-MBD/PIN1::PIN1-GFP* line was obtained by transforming *pAUR1::RFP-MBD* in *pB7m34GW* (Karimi et al. 2007) into the *pPIN1::PIN1-GFP* line (Benková et al. 2003) by floral dip and selection of transformants (Duchefa). The *pAUR1::RFP-MBD* construct was generated by Gateway cloning, combining *pAUR1* in *pDONRP4P1R* (Van Damme et al. 2011), *TagRFP* in *pDONR221* (Mylle et al. 2013), and the MBD of *MAP4* (Marc et al. 1998) in *pDONRP2P3R*. To generate *MBD* with the stop codon in *pDONRP2P3R*, it was amplified from *MBD* in *pDONR221* (Van Damme et al. 2004) with the following primers: MBD_FW_B2 (*GGGGACAGCTTTCTTGTACAAAGTGGCC*TCCCCAAGAAGAAGCAAAGG) and MBD_REV_stop_B3 (*GGGGACAACTTTGTATAATAAAGTTG*TTAACCTCCTGCAGGAAAGTGGCCA). The *GATA23::3xmCherry:SYP122* reporter for pericycle was constructed by cloning *3xmCherry* into *pGreen0179-SYP122* with KpnI and BamHI. Subsequently, the *GATA23* promoter (De Rybel et al. 2010) was amplified from genomic DNA (accession Columbia 0 [Col-0]) with primers *proGATA23KpnIfw GGGGTACCATAACTTTTCAATAATGGATC* and *proGATA23KpnIrv GGGGTACCCAAATAAAAAAAAACAATCTTAG* and cloned into *pGreen0179-3xmCherry:SYP122* with KpnI digestion, resulting in *pGreen0179-GATA23::3xmCherry:SYP122*. The construct was transformed into *pB7CASP1:γTIP:mCitrine* (Vermeer et al. 2014), and double-homozygous plants were selected.

Growth conditions

Seeds of *Arabidopsis* (accession Col-0) were plated on half-strength (0.5) Murashige and Skoog (MS) medium (Duchefa) with 1% (w/v) sucrose and 0.8% (w/v) agar (pH 5.7). The seeds were stratified for 2 d at 4°C. Seedlings were grown on vertically oriented plates in growth chambers under a 16-h light/8-h dark photoperiod at 21°C.

Pharmacological and hormonal treatments

Seedlings 5–6 d old were transferred onto solid MS medium with or without the indicated chemicals. The drugs and hormones used were 0.1 µM 1-naphthaleneacetic acid (NAA), 200 µM HU, and 10 µM PI. To inhibit lateral root initiation, seedlings were grown on 5 µM NPA for 5 d and maintained on the same NPA concentration during ablation and the following time-lapse experiment.

Confocal imaging and real-time analysis

For confocal microscopy images, the LSM 700 inverted confocal scanning microscope (Zeiss) and a conventional Axio Observer Z1 inverted microscope (Zeiss) were used. Pictures were taken with a 40× plan-apochromat water immersion objective. Fluorescence signals for GFP (excitation 488 nm, emission 500–530 nm) and PI (excitation 536 nm, emission 617 nm) were detected. YFP signals were observed with the GFP settings. Sequential scanning was used to avoid any interference between fluorescence channels (Marhavý and Benková 2015).

For laser cell ablation, 5- or 6-d-old seedlings were placed on chambered cover glasses (Nunc Lab-Tek) (Marhavý et al. 2014; Marhavý and Benková 2015) with roots oriented in the two xylem strain planes. After ECA of cells adjacent to pericycle cells (for details, see "UV Laser Setup for Cell-Specific Ablation"), the roots were scanned in 10-, 20-, or 30-min intervals for 10 to 15 h. The number of ECA-triggered pericycle cell divisions and their orientations (periclinal vs. anticlinal) were scored on recordings done for a 15-h period from the moment of ablation. At least 20 individual ablation events were analyzed. To detect cell death of ablated cells, the cells were stained with PI (see Supplemental Fig. S1). For image analyses, the ImageJ (National Institute of Health, http://rsb.info.nih.gov/ij) and Zeiss Zen 2011 programs were used. The statistical significance was evaluated with the Student's *t*-test.

UV laser setup for cell-specific ablation

The UV laser ablation setup was based on the layout (Colombelli et al. 2004) that uses a passively Q-switched solid-state 355-nm UV-A laser (Powerchip, Teem Photonics) with a pulse energy of 15 µJ at a repetition rate of 1 kHZ. With a pulse length of <350 psec, a peak power of 40 kW was obtained, of which typically <5% was used to cut tissue. The power was modulated with an acousto-optic modulator (AOM; Pegasus Optik, AA.MQl l0-43-UV). The laser beam diameter matched the size of the back aperture of the objectives by means of a variable zoom beam expander (Sill Optics), enabling diffraction-limited focusing while maintaining high transmission for objectives with magnifications in the 20× to 100× range. Point scanning was realized with a pair of high-speed galvanometric mirrors (Cambridge Technology, Lightning DS). To this end, the scanning mirrors were imaged into the image plane of the rear port of a conventional inverted microscope (Zeiss, Axio Observer Z1) with a telecentric f-θ objective (Jenoptik). To facilitate adjusting parfocality between the cutter and the spinning disk and compensate for the offset between the positions of the back planes of different objectives, the scan mirrors and the scan optics were mounted on a common translation stage. In the microscope reflector cube, a dichroic mirror reflected the UV light onto the sample but transmitted the fluorescence excitation and emission light. A UV-blocking filter in the emission path protected the camera and enabled simultaneous imaging and ablation. The AOM, the galvanometric mirrors, and a motorized stage (ASI, MS 2000) with a piezo-electric actuator on which the sample was mounted were computer controlled by custom-made software (Labview, National Instruments), enabling three-dimensional cuttings. The maximum field size for diffraction-limited cutting with little geometric distortion, high homogeneity of the intensity, and good field flatness was 300×300 m^2 for a 40× objective. The maximum depth was limited by the free-working distance of the objective used and the travel of the piezo-actuator (100 µm).

Acknowledgments

We thank Robert Hauschild for technical assistance with the UV laser ablation setup, Martine De Cock for help in preparing the manuscript, and Peter Doerner for sharing material. This work was supported by a European Research Council Starting Independent Research grant (ERC-2007-Stg-207362-HCPO to J.D.), Research Foundation-Flanders (G033711N to A.A.), and the

Austrian Science Fund (FWF01_I1774S to E.B.). P.M. is indebted to the Federation of European Biochemical Sciences for a Long-Term Fellowship. This research was supported by the Scientific Service Units (SSU) of Institute of Science and Technology Austria (IST-Austria) through resources provided by the Bioimaging Facility (BIF) and the Life Science Facility (LSF).

References

Beeckman T, De Smet I. 2014. Pericycle. *Curr Biol* **24:** R378–R379.

Beeckman T, Burssens S, Inzé D. 2001. The peri-cell-cycle in *Arabidopsis*. *J Exp Bot* **52:** 40–411.

Benková E, Michniewicz M, Sauer M, Teichmann T, Seifertová D, Jürgens G, Friml J. 2003. Local, efflux-dependent auxin gradients as a common module for plant organ formation. *Cell* **115:** 591–602.

Bielach A, Podlešáková K, Marhavý P, Duclercq J, Cuesta C, Müller B, Grunewald W, Tarkowski P, Benková E. 2012. Spatiotemporal regulation of lateral root organogenesis in *Arabidopsis* by cytokinin. *Plant Cell* **24:** 3967–3981.

Burk DH, Liu B, Zhong R, Morrison WH, Ye Z-H. 2001. A katanin-like protein regulates normal cell wall biosynthesis and cell elongation. *Plant Cell* **13:** 807–827.

Casimiro I, Marchant A, Bhalerao RP, Beeckman T, Dhooge S, Swarup R, Graham N, Inzé D, Sandberg G, Casero PJ, et al. 2001. Auxin transport promotes *Arabidopsis* lateral root initiation. *Plant Cell* **13:** 843–852.

Chen X, Grandont L, Li H, Hauschild R, Paque S, Abuzeineh A, Rakusová H, Benková E, Perrot-Rechenmann C, Friml J. 2014. Inhibition of cell expansion by rapid ABP1-mediated auxin effect on microtubules. *Nature* **516:** 90–93.

Cheng Y, Dai X, Zhao Y. 2006. Auxin biosynthesis by the YUCCA flavin monooxygenases controls the formation of floral organs and vascular tissues in *Arabidopsis*. *Genes Dev* **20:** 1790–1799.

Colombelli J, Grill SW, Stelzer EHK. 2004. Ultraviolet diffraction limited nanosurgery of live biological tissues. *Rev Sci Instrum* **75:** 472–478.

Colón-Carmona A, You R, Haimovitch-Gal T, Doerner P. 1999. Spatio–temporal analysis of mitotic activity with a labile cyclin–GUS fusion protein. *Plant J* **20:** 503–508.

De Rybel B, Vassileva V, Parizot B, Demeulenaere M, Grunewald W, Audenaert D, Van Campenhout J, Overvoorde P, Jansen L, Vanneste S, et al. 2010. A novel Aux/IAA28 signaling cascade activates GATA23-dependent specification of lateral root founder cell identity. *Curr Biol* **20:** 1697–1706.

De Smet I, Vanneste S, Inzé D, Beeckman T. 2006. Lateral root initiation or the birth of a new meristem. *Plant Mol Biol* **60:** 871–887.

Dharmasiri N, Dharmasiri S, Weijers D, Lechner E, Yamada M, Hobbie L, Ehrismann JS, Jürgens G, Estelle M. 2005. Plant development is regulated by a family of auxin receptor F box proteins. *Dev Cell* **9:** 109–119.

Dubrovsky JG, Doerner PW, Colón-Carmona A, Rost TL. 2000. Pericycle cell proliferation and lateral root initiation in *Arabidopsis*. *Plant Physiol* **124:** 1648–1657.

Dubrovsky JG, Gambetta GA, Hernández-Barrera A, Shishkova S, González I. 2006. Lateral root initiation in *Arabidopsis*: developmental window, spatial patterning, density and predictability. *Ann Bot* **97:** 903–915.

Dubrovsky JG, Sauer M, Napsucialy-Mendivil S, Ivanchenko MG, Friml J, Shishkova S, Celenza J, Benková E. 2008. Auxin acts as a local morphogenetic trigger to specify lateral root founder cells. *Proc Natl Acad Sci* **105:** 8790–8794.

Dubrovsky JG, Napsucialy-Mendivil S, Duclercq J, Cheng Y, Shishkova S, Ivanchenko MG, Friml J, Murphy AS, Benková E. 2011. Auxin minimum defines a developmental window for lateral root initiation. *New Phytol* **191:** 970–983.

Fischer K, Schopfer P. 1997. Interaction of auxin, light, and mechanical stress in orienting microtubules in relation to tropic curvature in the epidermis of maize coleoptiles. *Protoplasma* **196:** 108–116.

Fukaki H, Tameda S, Masuda H, Tasaka M. 2002. Lateral root formation is blocked by a gain-of-function mutation in the *SOLITARY-ROOT/IAA14* gene of *Arabidopsis*. *Plant J* **29:** 153–168.

Fukaki H, Nakao Y, Okushima Y, Theologis A, Tasaka M. 2005. Tissue-specific expression of stabilized SOLITARY-ROOT/IAA14 alters lateral root development in *Arabidopsis*. *Plant J* **44:** 382–395.

Geldner N, Dénervaud-Tendon V, Hyman DL, Mayer U, Stierhof Y-D, Chory J. 2009. Rapid, combinatorial analysis of membrane compartments in intact plants with a multicolor marker set. *Plant J* **59:** 169–178.

Hamada T. 2014. Microtubule organization and microtubule-associated proteins in plant cells. *Int Rev Cell Mol Biol* **312:** 1–52.

Heidstra R, Welch D, Scheres B. 2004. Mosaic analyses using marked activation and deletion clones dissect *Arabidopsis* SCARECROW action in asymmetric cell division. *Genes Dev* **18:** 1964–1969.

Heisler MG, Ohno C, Das P, Sieber P, Reddy GV, Long JA, Meyerowitz EM. 2005. Patterns of auxin transport and gene expression during primordium development revealed by live imaging of the *Arabidopsis* inflorescence meristem. *Curr Biol* **15:** 1899–1911.

Karimi M, Bleys A, Vanderhaeghen R, Hilson P. 2007. Building blocks for plant gene assembly. *Plant Physiol* **145:** 1183–1191.

Kepinski S, Leyser O. 2005. The *Arabidopsis* F-box protein TIR1 is an auxin receptor. *Nature* **435:** 446–451.

Laplaze L, Parizot B, Baker A, Ricaud L, Martinière A, Auguy F, Franche C, Nussaume L, Bogusz D, Haseloff J. 2005. GAL4-GFP enhance trap lines for genetic manipulation of lateral root development in *Arabidopsis thaliana*. *J Exp Bot* **56:** 2433–2442.

Laskowski M, Grieneisen VA, Hofhuis H, ten Hove CA, Hogeweg P, Marée AF, Scheres B. 2008. Root system architecture from coupling cell shape to auxin transport. *PLoS Biol* **6:** e307.

Lucas M, Kenobi K, von Wangenheim D, Voß U, Swarup K, De Smet I, Van Damme D, Lawrence T, Péret B, Moscardi E, et al. 2013. Lateral root morphogenesis is dependent on the mechanical properties of the overlaying tissues. *Proc Natl Acad Sci* **110:** 5229–5234.

Malamy JE, Benfey PN. 1997. Organization and cell differentiation in lateral roots of *Arabidopsis thaliana*. *Development* **124:** 33–44.

Marc J, Granger CL, Brincat J, Fisher DD, Kao T-h, McCubbin AG, Cyr RJ. 1998. A *GFP-MAP4* reporter gene for visualizing cortical microtubule rearrangements in living epidermal cells. *Plant Cell* **10:** 1927–1939.

Marhavý P, Benková E. 2015. Real-time analysis of lateral root organogenesis in *Arabidopsis*. *Bio Protoc* **5:** e1446.

Marhavý P, Vanstraelen M, De Rybel B, Ding Z, Bennett MJ, Beeckman T, Benková E. 2013. Auxin reflux between the endodermis and pericycle promotes lateral root initiation. *EMBO J* **32:** 149–158.

Marhavý P, Duclercq J, Weller B, Feraru E, Bielach A, Offringa R, Friml J, Schwechheimer C, Murphy A, Benková E. 2014.

Cytokinin controls polarity of PIN1-dependent auxin transport during lateral root organogenesis. *Curr Biol* **24:** 1031–1037.

Moreno-Risueno MA, Benfey PN. 2011. Time-based patterning in development: the role of oscillating gene expression. *Transcription* **2:** 124–129.

Mylle E, Codreanu M-C, Boruc J, Russinova E. 2013. Emission spectra profiling of fluorescent proteins in living plant cells. *Plant Methods* **9:** 10.

Swarup K, Benková E, Swarup R, Casimiro I, Péret B, Yang Y, Parry G, Nielsen E, De Smet I, Vanneste S, et al. 2008. The auxin influx carrier LAX3 promotes lateral root emergence. *Nat Cell Biol* **10:** 946–954.

Takesue K, Shibaoka H. 1999. Auxin-induced longitudinal-to-transverse reorientation of cortical microtubules in nonelongating epidermal cells of azuki bean epicotyls. *Protoplasma* **206:** 27–30.

Ubeda-Tomás S, Federici F, Casimiro I, Beemster GTS, Bhalerao R, Swarup R, Doerner P, Haseloff J, Bennett MJ. 2009. Gibberellin signalling in the endodermis controls *Arabidopsis* root meristem size. *Curr Biol* **19:** 1194–1199.

Ulmasov T, Murfett J, Hagen G, Guilfoyle TJ. 1997. Aux/IAA proteins repress expression of reporter genes containing natural and highly active synthetic auxin response elements. *Plant Cell* **9:** 1963–1971.

Uyttewaal M, Burian A, Alim K, Landrein B, Borowska-Wykret D, Dedieu A, Peaucelle A, Ludynia M, Traas J, Boudaoud A, et al. 2012. Mechanical stress acts via katanin to amplify differences in growth rate between adjacent cells in *Arabidopsis*. *Cell* **149:** 439–451.

Van Damme D, Van Poucke K, Boutant E, Ritzenthaler C, Inzé D, Geelen D. 2004. In vivo dynamics and differential microtubule-binding activities of MAP65 proteins. *Plant Physiol* **136:** 3956–3967.

Van Damme D, De Rybel B, Gudesblat G, Demidov D, Grunewald W, De Smet I, Houben A, Beeckman T, Russinova E. 2011. *Arabidopsis* α Aurora kinases function in formative cell division plane orientation. *Plant Cell* **23:** 4013–4024.

Vanneste S, De Rybel B, Beemster GTS, Ljung K, De Smet I, Van Isterdael G, Naudts M, Iida R, Gruissem W, Tasaka M, et al. 2005. Cell cycle progression in the pericycle is not sufficient for SOLITARY ROOT/IAA14-mediated lateral root initiation in *Arabidopsis thaliana*. *Plant Cell* **17:** 3035–3050.

Vermeer JEM, von Wangenheim D, Barberon M, Lee Y, Stelzer EHK, Maizel A, Geldner N. 2014. A spatial accommodation by neighboring cells is required for organ initiation in *Arabidopsis*. *Science* **343:** 178–183.

Vineyard L, Elliott A, Dhingra S, Lucas JR, Shaw SL. 2013. Progressive transverse microtubule array organization in hormone-induced *Arabidopsis* hypocotyl cells. *Plant Cell* **25:** 662–676.

Young CW, Hodas S. 1964. Hydroxyurea: inhibitory effect on DNA metabolism. *Science* **146:** 1172–1174.

Žádníková P, Petrášek J, Marhavý P, Raz V, Vandenbussche F, Ding Z, Schwarzerová K, Morita MT, Tasaka M, Hejátko J, et al. 2010. Role of PIN-mediated auxin efflux in apical hook development of *Arabidopsis thaliana*. *Development* **137:** 607–617.

Zhao Y, Christensen SK, Fankhauser X, Cashman JR, Cohen JD, Weigel D, Chory J. 2001. A role for flavin monooxygenase-like enzymes in auxin biosynthesis. *Science* **291:** 306–309.